

A non-empirical free volume viscosity model for alkane lubricants under severe pressures

Kerstin Falk,¹ Daniele Savio,¹ and Michael Moseler^{1,2}

¹*Fraunhofer IWM, Wöhlerstr. 11, 79108 Freiburg, Germany*

²*Institute of Physics, University of Freiburg, Herrmann-Herder-Str. 3, 79104 Freiburg, Germany*

Viscosities η and diffusion coefficients D_s of linear and branched alkanes at high pressures $P < 0.7$ GPa and temperatures $T = 500\text{--}600$ K are calculated by equilibrium molecular dynamics (EMD). Combining Stokes-Einstein, free volume and random walk concepts results in an accurate viscosity model $\eta(D_s(P, T))$ for the considered P and T. All model parameters (hydrodynamic radius, random walk step size and attempt frequency) are defined as microscopic ensemble averages and extracted from EMD simulations rendering $\eta(D_s(P, T))$ a parameter-free predictor for lubrication simulations.

Knowledge-based design and optimization of liquid lubricants require a quantitative modelling of their rheological properties under relevant tribological conditions [1]. For instance, lubricants in roller element bearing and gear applications are subject to pressures of the order of GPa [2]. Traditional empirical viscosity models (such as Barus or Roelands equation) fail to describe $\eta(P)$ over the relevant pressure range [3] indicating that improved viscosity models for the extreme pressure regime [4, 5] should be based on physical insights [6]. A promising approach employs the Stokes-Einstein relation [7]

$$D_s = k_B T / (n \pi \eta R_h) \quad (1)$$

that connects the viscosity with the self-diffusion coefficient D_s . Here, R_h denotes the hydrodynamic radius and n lies between the slip and no-slip hydrodynamics limits, 4 and 6. The applicability of Eq. (1) on a microscopic level has been theoretically motivated and is well established under normal conditions [8, 9], also for non-spherical molecules if R_h is considered a free parameter. However, a breakdown of Stokes law has been observed in various dense liquids, including molecular glass formers [10, 11]. The mechanism of this breakdown is still subject to extensive research, mostly focused on densification obtained by supercooling [12–14]. This raises the question whether Eq. (1) remains valid for liquids which are densified by pressurisation instead of cooling.

In this letter, EMD simulations are utilized to validate Eq. (1) for linear and branched alkanes (constituents of ordinary lubricant base stock) for a pressure and temperature range representing typical tribological high load applications. We suggest a microscopic definition of

$$R_h = \sqrt{\langle a \rangle / \pi} \quad (2)$$

by introducing an EMD averaged molecular cross section $\langle a \rangle$. This represents an important step towards a parameter-free structure-property relationship (SPR) relating molecular structure with macroscale viscosities.

Employing Eq. (1) necessitates an additional SPR for D_s . Here, we utilize the free volume (FV) concept [15, 16]

$$D_s = D_0 \exp(-v_c/v_f). \quad (3)$$

with the mean FV per molecule v_f and the critical volume v_c . Note, that since v_f is determined by the lubricant density ρ an equation of state $\rho(P)$ is required to arrive at a pressure dependent viscosity law.

Although widely used for soft matter systems [17–19], the FV concept is being challenged due to concerns about the relevance of FV compared to energetic effects and about the physical interpretation of the free parameters D_0 and v_c [20–24]. We show in the second part of this letter that Eq. (3) can be applied to our alkane lubricants and suggest microscopic definitions of D_0 and v_c . The latter relies on the observation that self-diffusion can be considered a random walk of a molecule’s center of mass (COM) with step length and attempt frequency determined by EMD simulations.

Two linear alkanes and three poly- α -olefines (PAO) (for structures see Fig.1a) are modelled with the all-atom optimized potentials for liquid simulations (AA-OPLS) [25]. The EMD of these lubricants is simulated within a constant volume subject to periodic boundary conditions for densities ranging roughly from 470 to 850 kg/m³. Time integration is performed employing the LAMMPS software suite [26, 27] with timestep 0.5 fs, and a Nosé-Hoover thermostat with relaxation time 0.1 ps [28, 29]. Viscosities η are determined via the Green-Kubo formalism and self-diffusion coefficients D_s via the mean squared displacement (MSD) [9] (see supp. Figs. S1/2).

As shown in Fig.1b, results for η and D_s vary over 3 orders of magnitude and are fully compatible with Eq. (1) (assuming slip boundary conditions $n=4$ [8, 9]). A parameter-free quantitative agreement is achieved by introducing the hydrodynamic radius via Eq. (2) as follows. Since the Stokes drag on macroscopic solid objects with slippery surfaces scales with the object’s cross section in the direction of a displacement [30], we calculate a directional molecular cross section a as indicated in Fig.1c. To each molecule a volume v_{mol} is assigned using a coarse grained hard sphere approach based on a CH_X ($X = 1, 2, 3$) united atom representation [31] (see details in supp. Fig. S3). Then the molecule is displaced over a short distance ε and its effective cross section area

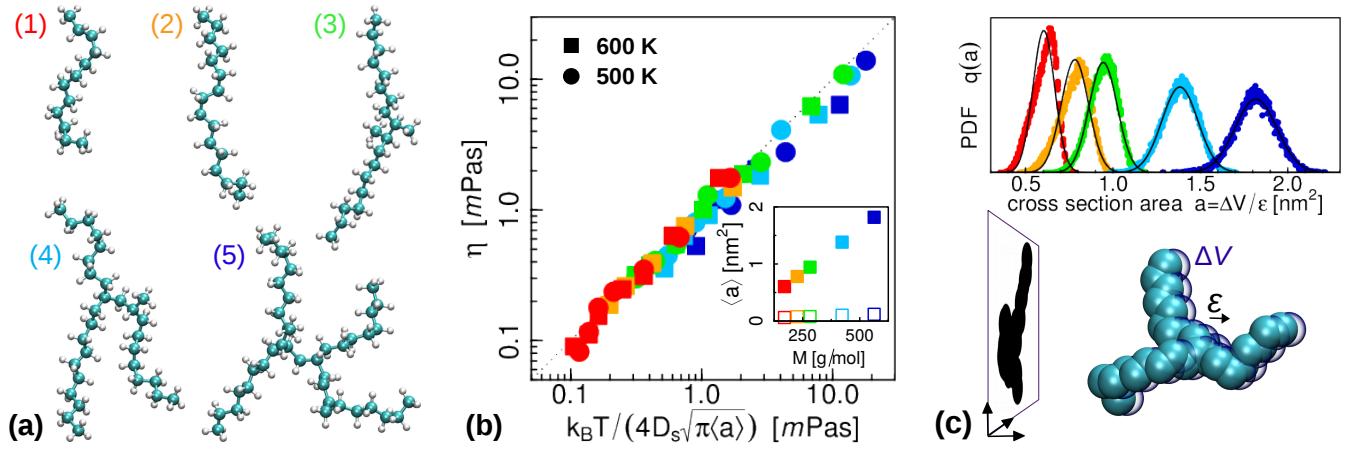


FIG. 1. Stokes radius of complex molecules. (a) Considered molecular structures: *n*-dodecane (1, red), *n*-hexadecane (2, orange), PAO-C₁₀-dimer (3, green), PAO-C₁₀-trimer (4, light blue), and PAO-C₁₀-tetramer (5, dark blue) (b) Shear viscosity η and self diffusion coefficient D_s under extreme pressure (up to 0.7 GPa) and temperature (■/● 600/500 K) from EMD simulations: Quantitative agreement with the Stokes-Einstein relation Eq.(1), assuming a slip boundary condition ($n=4$) and a molecule radius $R_h = \sqrt{\langle a \rangle / \pi}$ with $\langle a \rangle$ the molecule's mean cross section area (inset: ■ mean $\langle a \rangle$, □ standard deviation). (c) Definition of the configuration dependent cross section area $a := \Delta V / \varepsilon$ (ΔV newly occupied volume after a small virtual displacement ε), and resulting distributions $q(a)$; for comparison, lines show Gaussian distributions.

is defined by $a = \Delta V / \varepsilon$, where ΔV is the newly occupied volume. Finally, the mean cross section is obtained by $\langle a \rangle = \int a q(a) da$, where $q(a)$ is the probability for the molecule to have a configuration with cross section a . Interestingly, $\langle a \rangle$ scales linearly with the molecule size, despite the different morphologies (i.e. number of branches in alkanes - see inset in Fig. 1b). This scaling can be rationalized by a cylindrical shape estimate of long alkane chains, neglecting the contribution of chain ends and knots (supp. Fig. S4).

After having established a parameter-free relation between η and D_s , we now focus on the diffusive motion of the alkanes. Fig. 2a shows part of a C₁₀-trimer COM trajectory with a behaviour which is characteristic of a caging effect. The COM position oscillates within a compact volume due to confinement by the neighboring molecules (snapshots 1,3,5 of Fig. 2a). Elementary diffusion steps (EDS) take place via occasional irreversible translations (indicated by red arrows in snapshots 2,4,6 of Fig. 2a). The FV ansatz leading to Eq. (3) assumes that the probability for an EDS is given by $p(v_c) = \exp(-v_c/v_f)$. Here, v_c is the critical void size in the cage formed by a molecule's neighbours allowing for an irreversible COM jump. Following the simple argument that this void has to accommodate the molecule, the critical volume v_c is expected to be of the order of the hard core molecule volume v_{mol} . Note, that $p(v_c)$ depends parametrically on the mean free volume per molecule $v_f = v - v_{mol}$, where v denotes the molar volume [16].

Indeed, the self diffusion coefficient follows the form Eq. (3), as shown in Fig. 2b, where lines are best fits for

the 600 K data. Fig. 2c displays the dependence of the fit parameters \tilde{v}_c and \tilde{D}_0 on the size of the molecules. Surprisingly, the critical volume is about 3 times larger than v_{mol} in contradiction to the simple argument stated above. An alternative interpretation of v_c is based on the following consideration. To perform an EDS, a molecule needs to move from its cage center to a void in the cage wall. The necessary critical volume for this displacement over the cage size r_c is then $r_c \cdot a$ with a the molecule's cross section. For constant a and r_c , the diffusion process could then be pictured as a random walk with stepsize r_c and step frequency $1/\Delta t$. The latter is the product of an attempt frequency $1/\tau_0$ and the success probability $\exp(-r_c a/v_f)$ resulting in

$$D_s(a, r_c) = r_c^2 / (6\Delta t) = r_c^2 / (6\tau_0) \exp(-r_c a/v_f). \quad (4)$$

However, both a and r_c depend a priori on the molecules' configurations with respect to the direction of the EDS. Fluctuating shapes and distances in molecular fluids result in a probability distribution $q(a, r_c)$ for a and r_c that determine the diffusion coefficient $D_s(a, r_c)$ in a certain direction and thus the total diffusion coefficient is $D_s = \int D_s(a, r_c) q(a, r_c) da dr_c$. In the following, we demonstrate by sampling $q(a, r_c)$ over all possible configurations and orientations that the first moments $\langle a \rangle = \int a q(a, r_c) da dr_c$ and $\langle r_c \rangle = \int r_c q(a, r_c) da dr_c$ dominate the diffusion process:

$$D_s \approx \langle r_c \rangle^2 / (6\tau_0) \exp(-\langle r_c \rangle \langle a \rangle / v_f). \quad (5)$$

For a given configuration, Eq.(4) implies a direction dependent stepsize and success probability for an individual

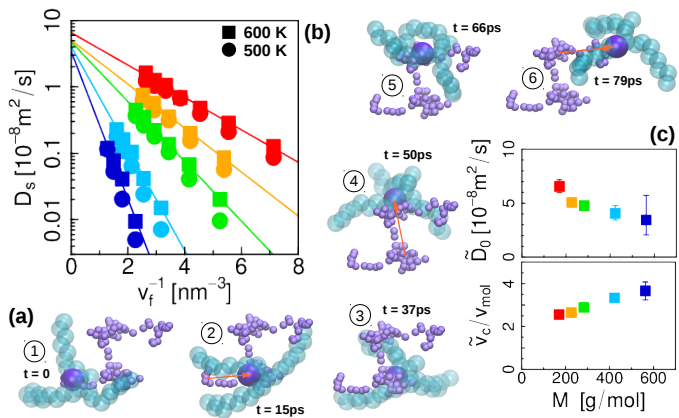


FIG. 2. Dependence of diffusion on free volume. (a) Part of a C₁₀-trimer trajectory within bulk fluid at 0.6 MPa. Light blue: C-atoms; large dark blue: COM position; small violet: all COM positions (every 1 ps during 85 ps). The COM diffusive motion (arrows) can be described by a random walk between caged positions due to the confining presence of the surrounding molecules (not displayed). (b) Self diffusion coefficient D_s vs. inverse of the mean free volume per molecule $v_f = v - v_{mol}$ (colors as in Fig. 1, ■/● 600/500 K). Lines are best fits of $D_s = D_0 \exp(-v_c/v_f)$ on 600 K data. (c) Fit results \tilde{D}_0 and \tilde{v}_c ; errorbars: 68%-confidence interval.

EDS. To study this anisotropy we consider an auxiliary system of preferentially oriented alkanes immersed in a bath of unconstrained molecules. This artificial test situation is realized for *n*-hexadecane at two different densities by applying opposing external forces ± 0.05 eV/Å to the head and tail carbon atoms of 2.6% of the molecules (Fig. 3a). The resulting preferential orientation leads to a permanently anisotropic cross section $\langle a(\theta) \rangle$ (Fig. 3b) and cage radius $\langle r_c(\theta) \rangle$ (red dots in Fig. 3c), where θ denotes the angle between the applied forces and the EDS direction. Here, $\langle a(\theta) \rangle$ was calculated as previously defined (see Fig. 1c) for a given direction θ . Lacking an unambiguous definition of $\langle r_c(\theta) \rangle$, a pragmatic estimate was based on the direction dependent radial distribution function $g_{COM}(\theta, r)$ of the molecules' COM (Fig. 3c) via $g_{COM}(\theta, \langle r_c(\theta) \rangle) = 1$. In the same spirit, the isotropic cage size $\langle r_c \rangle$ (circle in Fig. 3c) was determined from the isotropic radial distribution function $g_{COM}(r)$ (bold line in Fig. 3c). Note, that this value is close to the result obtained via $\langle r_c \rangle = \int \langle r_c(\theta) \rangle d \cos \theta$.

As expected the preferentially oriented molecules exhibit a pronounced anisotropy in the MSD $\langle r^2(\theta) \rangle$ (Fig. 3d) and consequently in the diffusion coefficient $D_s(\theta)$. Interestingly, the mean diffusion coefficient $D_s = (D_s(\theta = 0) + 2D_s(\theta = \pi/2))/3$ is equal to the isotropic diffusion coefficient of the unperturbed molecules, confirming that diffusion is given by an average over all directions with respect to the main axis of a hexadecane molecule. Most importantly however, $D_s(\theta)$ scales with

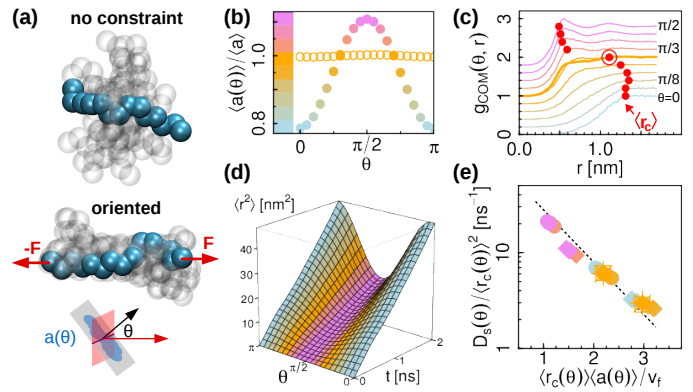


FIG. 3. Diffusion of artificially oriented *n*-hexadecane molecules in an unconstrained bath. (a) Superimposed configurations of one randomly chosen bath and one oriented molecule ($\pm F$ applied along $\theta = 0; \pi$, COM motion subtracted, 1 frame/ns). (b) mean cross section $\langle a(\theta) \rangle$ for un/constrained (○/●) molecules, unperturbed value $\langle a \rangle$ see Fig. 1. (c) θ -dependent COM radial distribution function (shifted for better visibility) with estimate of cage radius $\langle r_c(\theta) \rangle$ (●); same for isotropic COM-RDF of bath molecules (bold line, ○). (d) Anisotropic MSD for oriented molecules in least dense system. (e) Anisotropic self diffusion coefficient $D_s(\theta)$ (2 different densities ●, ◆) normalized with static structure properties according to Eq.(5); direction averaged values $D_s = (D_s(0) + 2D_s(\pi/2))/3$, isotropic D_s of bath molecules and of unperturbed systems (×, +, □) are identical.

the respective static structure properties as predicted by Eq.(5) validating the applicability of a FV ansatz on the microscopic level of an EDS (Fig. 3e).

Comparing Eq.(3) with (5) leads to $D_0 = \langle r_c \rangle^2 / (6\tau_0)$ and $v_c = \langle r_c \rangle \langle a \rangle$. Indeed, applying the above structure evaluation for $\langle a \rangle$ (inset in Fig. 1b) and $\langle r_c \rangle$ (Fig. 4a) to the unperturbed systems of all 5 fluid types reveals that the product $v_c = \langle r_c \rangle \langle a \rangle$ agrees well with the fitted critical volumes \tilde{v}_c (Fig. 4a inset). Both, $\langle a \rangle$ and $\langle r_c \rangle$ are only weakly dependent on density and temperature (supp. Figs. S5/6) and can be conveniently estimated from an EMD simulation for a single ρ and T .

The remaining free parameter τ_0 (time between random walk attempts) can be interpreted as the time scale for structure decorrelation in the molecule/cage system. The connection between structural relaxation, diffusion and viscosity is subject of ongoing research [33], and fully unravelling the underlying mechanisms goes far beyond the scope of this work. Nevertheless, as a starting point we consider the time autocorrelation function $\langle \mathbf{e}(0) \cdot \mathbf{e}(t) \rangle$ of the molecules' end-to-end vector orientation $\mathbf{e}(t)$ (see Fig. 4b) to quantify the intramolecular structure decorrelation. For long hydrocarbon chains, $\langle \mathbf{e}(0) \cdot \mathbf{e}(t) \rangle$ is well described by a double exponential function [34]

$$\langle \mathbf{e}(0) \cdot \mathbf{e}(t) \rangle = C e^{-t/\tau_\alpha} + (1 - C) e^{-(t/\tau_\beta)^b} \quad (6)$$

with two separate characteristic decay times τ_α and τ_β .

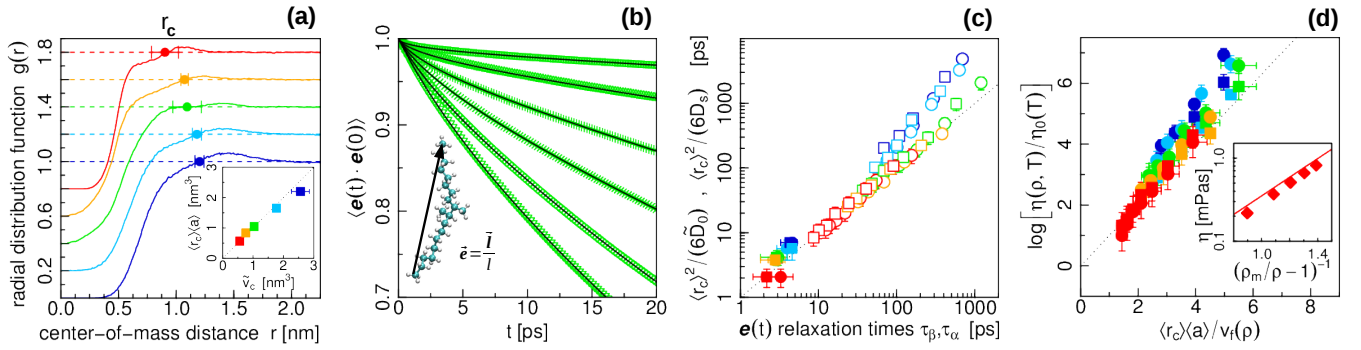


FIG. 4. Scaling of viscosity and self diffusion coefficient with molecule structure properties [Colors as in Fig. 1]. (a) COM radial distribution functions (lines, shifted for better visibility) with estimate of $\langle r_c \rangle$ (\bullet); *inset*: fit result for the critical volume \tilde{v}_c (see Fig. 2) vs. $\langle r_c \rangle \langle a \rangle$ ($\langle a \rangle$ mean cross section area, see Fig. 1). (b) Time autocorrelation function of the C₁₀-dimer end-to-end vector orientation $\mathbf{e}(t)$ for all considered densities at 500 K (symbols) with fits of Eq. (6) (lines); all other molecules in supp. Fig. S7. (c) Correlation times τ_β and τ_α (full/empty symbols) vs. predicted attempt and waiting time of the random walk diffusion model $\tau_0 = \langle r_c \rangle^2 / (6D_0)$ and $\Delta t = \langle r_c \rangle^2 / (6D_s)$, respectively; data for τ_β shows the mean value from all densities. (d) Scaled viscosity $\log(\eta/\eta_0)$ with $\eta_0 = 1.5k_B T \tau_\beta / (\langle r_c \rangle^2 \sqrt{\pi \langle a \rangle})$ vs. ratio of critical to free volume $\langle r_c \rangle \langle a \rangle / v_f$ (no free parameter); *inset*: Experimental data for *n*-dodecane at $T = 473$ K from Ref. [32] (\blacklozenge) and prediction from simulations (line).

On the one hand, a long time decay is observed on the time scale of the diffusion process $\tau_\alpha \approx \Delta t = r_c^2 / (6D_s)$, ranging from 10 ps - 1 ns. On the other hand, τ_β is of the order of 1 – 10 ps and is insensitive to the fluid density (within statistical uncertainties, see supp. Fig. S7). This β -relaxation time fits well with the expected attempt frequency for the random walk $\tau_\beta \approx \tau_0 = r_c^2 / (6D_0)$ as illustrated in Fig. 4c, which suggests it as a good measure for the relevant structure decorrelation on short times.

The presented results are further validated in a series of scaling tests with modified model parameters for both intra- and intermolecular interactions (supp. Fig. S8). In particular, the strength of nonbonded interactions has little influence, but a scaling of the atomic radii σ_{LJ} results in strong variations of the diffusivity caused by the exponential term in Eq. (5). Moreover, the prefactor D_0 is sensitive to variations of the energy barrier for bond rotation, which influences intramolecular relaxations. All scaling tests are also in quantitative agreement with the Stokes-Einstein relation, supporting our definition of a hydrodynamic radius in Eq. (2).

Finally, combining Eqs.(1), (2) and (5) the viscosity can be expressed as a function of density

$$\log \frac{\eta(T, \rho)}{\eta_0(T)} = \frac{\langle r_c \rangle \langle a \rangle}{v_{mol}} (\rho_m / \rho - 1)^{-1} \quad (7)$$

with $\rho_m = M/v_{mol}$ the maximum hypothetical density for zero free volume ($1 - v_f/v = \rho/\rho_m$; supp. Fig. S4). Apart from the density, the r.h.s. contains only equilibrium structure properties, namely the molecules' volume v_{mol} , mean cross section $\langle a \rangle$ and mean next neighbor distance $\langle r_c \rangle$. The temperature dependence of η enters via $\eta_0(T) = 1.5k_B T \tau_0(T) / (r_c^2 \sqrt{\pi \langle a \rangle})$. By employing Eq.(7) and identifying τ_0 with τ_β a parameter free rescaling

of the simulated viscosities can be established (Fig. 4d). This scaling law can also be applied to experimental high T and P viscosity data for *n*-dodecane [32]. We find a good agreement of the experimental data with our parameter-free viscosity model Eq. (7) (inset of Fig. 4d).

To conclude, a combination of basic random walk and FV theory fully describes the self diffusion mechanism of long alkane chains, linear and branched alike, in the high T and P regime. A crucial part of the presented work is the introduction of the mean cross section $\langle a \rangle$ and mean cage size $\langle r_c \rangle$ as novel molecule shape parameters. While $\langle a \rangle$ establishes a quantitative link between viscosity and self diffusion via the Stokes-Einstein relation, $\langle a \rangle$ and $\langle r_c \rangle$ allow for a parameter-free density scaling of both transport coefficients. The viscosity model can be directly implemented in density-based Reynolds-solvers [35] and will contribute to a new cutting-edge simulation tool for tribological applications. The proposed shape parameters also opens new possibilities to quantify the role of molecular structure on rheology in anisotropic situations, such as shear thinning [36, 37] or in nanometer-thin boundary lubrication films [38]. Our approach might also be useful for other soft materials, such as self assembled membranes [17, 18], polymer-solvent systems [19] or adsorbates in nanopores [39].

The authors gratefully acknowledge funding by the industrial partners of the MikroTribologie Centrum μ TC (Karlsruhe, Germany), computing time within project HFR14 at NIC Jülich and useful discussions with L. Joly, S. Kapfer and L. Bocquet.

-
- [1] S. Bair, *High Pressure Rheology for Quantitative Elastohydrodynamics*, 1st ed. (Elsevier, 2007).
- [2] H. Spikes, Proceedings of the Institution of Mechanical Engineers, Part J: Journal of Engineering Tribology **208**, 3 (1994).
- [3] S. Bair and C. Kottke, Tribology Transactions **46**, 289 (2003).
- [4] S. Bair, C. Mary, N. Bouscharain, and F. Vergne, Proc. IMechE Part J: J Engineering Tribology **227**, 1056 (2013).
- [5] J. J. De la Porte and C. A. Kossack, Fuel **136**, 156 (2014).
- [6] P. Vergne and S. Bair, Tribology Letters **54**, 1 (2014).
- [7] A. Einstein, Annalen der Physik **322**, 549 (1905).
- [8] R. Zwanzig and M. Bixon, Phys. Rev. A **2**, 2005 (1970).
- [9] J.-P. Hansen and I. R. McDonald, *Theory of simple liquids*, 4th ed. (Academic Press, Oxford, 2013).
- [10] P. Bordat, F. Affouard, M. Descamps, and F. Müller-Plathe, J. Phys.: Condens. Matter. **15**, 5397 (2003).
- [11] J. Brillo, A. I. Pommrich, and A. Meyer, Phys. Rev. Lett. **107**, 165902 (2011).
- [12] P. Charbonneau, Y. Jin, G. Parisi, and F. Zamponi, P. Natl. Acad. Sci. USA **111**, 15025 (2014).
- [13] P. Henritzi, A. Bormuth, F. Klameth, and M. Vogel, J. Chem. Phys. **143**, 164502 (2015).
- [14] T. Kawasaki and K. Kim, Sci. Adv. **3** (2017), 10.1126/sciadv.1700399.
- [15] A. K. Doolittle, J. Appl. Phys. **22**, 1471 (1951).
- [16] M. H. Cohen and D. Turnbull, J. Chem. Phys. **31**, 1164 (1959).
- [17] P. F. F. Almeida, W. L. C. Vaz, and T. E. Thompson, Biochemistry **31**, 6739 (1992).
- [18] M. Javanainen, L. Monticelli, J. B. de la Serna, and I. Vattulainen, Langmuir **26**, 15436 (2010).
- [19] J. S. Vrentas and C. M. Vrentas, *Diffusion and mass transfer*, 1st ed. (CRC Press Taylor & Francis Group, 2012).
- [20] J. S. Vrentas and C. M. Vrentas, J. Polym. Sci. B: Pol. Phys. **41**, 501 (2003).
- [21] E. Falck, Biophys. J. **89** (2005), 10.1529/biophysj.105.065714.
- [22] B. A. Betancourt, P. Z. Hanakata, F. W. Starr, and J. F. Douglas, P. Natl. Acad. Sci. USA **112**, 2966 (2015).
- [23] L. Berthier and G. Biroli, Rev. Mod. Phys. **83**, 587 (2011).
- [24] V. Jadhao and M. O. Robbins, P. Natl. Acad. Sci. USA **114**, 7952 (2017).
- [25] W. L. Jorgensen, D. S. Maxwell, and J. Tirado-Rives, J. Am. Chem. Soc. **118**, 11225 (1996).
- [26] S. Plimpton, J. Comput. Phys. **117**, 1 (1995).
- [27] <http://lammps.sandia.gov>, *Large-scale Atomic/Molecular Massively Parallel Simulator*.
- [28] M. P. Allen and D. J. Tildesley, *Computer simulation of liquids*, 1st ed. (Clarendon Press, Oxford, 1989).
- [29] D. Frenkel and B. Smit, *Understanding molecular simulation: From algorithms to applications (Computational Science Series, Vol 1)*, 2nd ed. (Academic Press, 2001).
- [30] D. Leith, Aerosol Sci. Tech. **6**, 153 (1987).
- [31] M. G. Martin and J. I. Siepmann, J. Phys. Chem. B **102**, 2567 (1998).
- [32] D. R. Caudwell, J. P. M. Trusler, V. Vesovic, and W. A. Wakeham, Int. J. Thermophys. **25**, 1339 (2004).
- [33] X. Ma, Z. S. Davidson, T. Still, R. J. S. Ivancic, S. S. Schoenholz, A. J. Liu, and A. G. Yodh, Phys. Rev. Lett. **122**, 028001 (2019).
- [34] H. Morhenn, S. Busch, and T. Unruh, J. Phys.: condens. Matter **24** (2012), 10.1088/0953-8984/24/37/375108.
- [35] H. G. Elrod, J. of Lubrication Tech. **103**, 350 (1981).
- [36] P. Liu, J. Lu, H. Yu, N. Ren, F. E. Lockwood, and Q. J. Wang, J. Chem. Phys. **147**, 084904 (2017).
- [37] T. S. Ingebrigtsen and H. Tanaka, P. Natl. Acad. Sci. USA **115**, 87 (2018).
- [38] I. Rosenhek-Goldian, N. Kampf, A. Yeredor, and J. Klein, P. Natl. Acad. Sci. USA **112**, 7117 (2015).
- [39] K. Falk, B. Coasne, R. Pellenq, F.-J. Ulm, and L. Bocquet, Nat. Commun. **6** (2015), 10.1038/ncomms7949.